Application of optimal control theory to inverse simulation of car handling

Document status and date:
Published: 01/01/1996

Document Version:
Publisher's PDF, also known as Version of Record (includes final page, issue and volume numbers)

Please check the document version of this publication:

• A submitted manuscript is the version of the article upon submission and before peer-review. There can be important differences between the submitted version and the official published version of record. People interested in the research are advised to contact the author for the final version of the publication, or visit the DOI to the publisher's website.
• The final author version and the galley proof are versions of the publication after peer review.
• The final published version features the final layout of the paper including the volume, issue and page numbers.

Link to publication

Application of Optimal Control Theory to Inverse Simulation of Car Handling

J.P.M. HENDRIKX, T.J.J. MEIJLINK and R.F.C. KRIENS *

SUMMARY

The application of Optimal Control Theory to time-optimal inverse simulation of car handling was investigated. Time-optimal inverse simulation of car handling involves the calculation of driver actions required to perform specified manoeuvres, in as short a time as possible. Driver actions consist of time-histories of front wheel steer rate and longitudinal force. Optimal time-histories of these quantities were calculated using the Gradient method after formulating the problem as one of optimal control. Simulation results are presented for two different cars performing similar lane-changes. These results show significant differences in necessary driver actions for different cars and demonstrate the suitability of the approach taken.

1. INTRODUCTION

Inverse simulation of car handling differs from traditional open-loop simulation because the driver actions are calculated from prescribed car manoeuvres instead of vice versa. Because in most real driving situations the car manoeuvre is prescribed, results from inverse simulation models promise better correlation with reality than results from open-loop simulation models. In literature, various inverse models for calculating the driver actions have been proposed [1–5]. The main differences between these models lie in the way the car is modeled and in the way the manoeuvre is defined. The car is represented as a two-dimensional two-wheel model [1–4] or as a three-dimensional model with either linear or non-linear tire characteristics. The manoeuvre is defined either by the time-histories of the car state variables that have to be achieved almost exactly [2,5], by a path that has to be followed closely [3,4] or by a road the car has to stay on [1]. In the latter two cases, additional criteria are defined to eliminate the possiblity of multiple solutions. In [3,4], a criterion related to driver effort is minimized, while in [1] the time required to complete the manoeuvre is minimized.

For the research presented here, the car is represented as a two-dimensional four-wheel model. The tire model is non-linear and is compensated for traction influences. The manoeuvre is defined by a road the car has to stay on while the

* Laboratory for Automotive Engineering, Eindhoven University of Technology, P.O. Box 513, 5600 MB, Eindhoven, The Netherlands.

driver actions are front wheel steer rate and longitudinal force. To eliminate the uncertainties about driver behaviour and to exclude the possibility of multiple solutions, the car is required to perform the manoeuvre in as short a time as possible. Hence, the problem is that of determining the driver actions that will allow a car to perform the manoeuvre as quick as possible, whilst staying on the specified road. This problem was solved by applying the Gradient method after formulating it as one of optimal control. The general formulation of an optimal control problem is that of determining the time-histories of the control variables that will cause a dynamic system to be transferred from an initial state to a final state whilst minimizing a functional and without violating any constraints. Here, the dynamic system is the car, the control variables are the driver actions, the functional is the time required to complete the manoeuvre, and the constraints are the road and the car's performance limits. These quantities are discussed in detail and results of two cases are presented. In these cases, a rear wheel drive and a front wheel drive car were required to perform a lane-change. The results of these simulations not only show the proper functioning of the model, they also show the significant effect of drive and brake torques on tire saturation, during minimum-time cornering.

2. MODELING

The optimal control formulation of the inverse simulation problem requires: a set of equations representing the dynamic behaviour of the car i.e. the equations of motion, a criterion representing the car's performance i.e. the cost functional, a set of data representing the possible limits on the controls i.e. the control constraints, and a set of data representing the road the car is to stay on i.e. the state constraints.

2.1. Equations of Motion
The car is modeled as a single mass with yaw, lateral, and longitudinal degrees of freedom. (see Fig. 1)
Its equations of motion are

$$\dot{x}_1 = x_2 \tag{1}$$

$$\dot{x}_2 = \left((F_{y1} + F_{y2})l_f - (F_{y3} + F_{y4})l_r\right)/I \tag{2}$$

$$\dot{x}_3 = \left(F_{y1} + F_{y2} + F_{y3} + F_{y4}\right)/M - x_2 x_4 \tag{3}$$

$$\dot{x}_4 = \left((K_f + K_r)1000u_2 - F_a\right)/M + x_2 x_3 \tag{4}$$

$$\dot{x}_5 = x_4 \sin(x_1) + x_3 \cos(x_1) \tag{5}$$

$$\dot{x}_6 = x_4 \cos(x_1) - x_3 \sin(x_1) \tag{6}$$
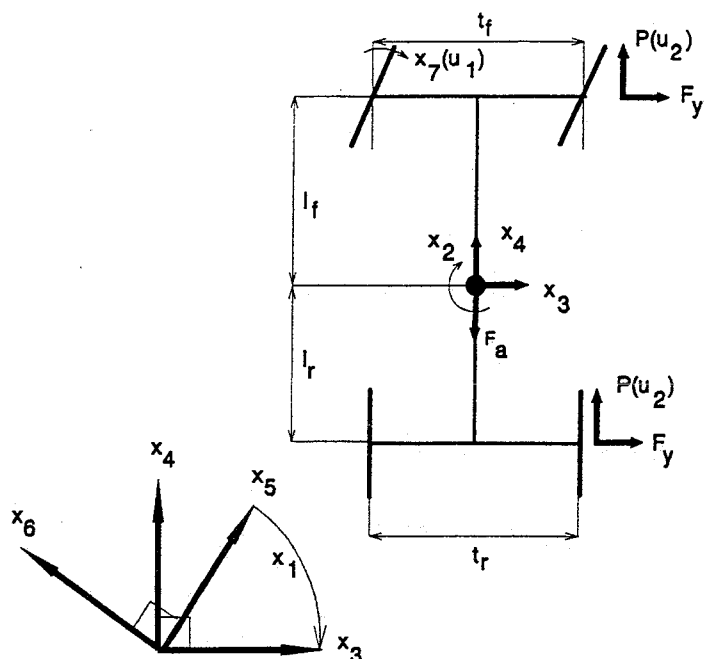
$$\dot{x}_7 = u_1 \tag{7}$$

Fig. 1. Schematic representation of vehicle model with sign conventions.

All quantities used in these equations are listed in Tables 1 and 2 except for the factor 1000 in Equation (4). This factor compensates for the expression of drive and brake forces in kilo Newtons which, in the interest of the optimization algorithm, allows both controls to have the same order of magnitude.

Table 1. Nomenclature.

A	car frontal area	m^2
F	tire lateral force, excluding traction effects	N
F_a	aerodynamic drag	N
F_y	tire lateral force, including traction effects	N
F_z	tire normal force	N
g	gravitational acceleration (9.81)	m/s^2
$l_{f,r}$	distance from center of front and rear axles to centre of gravity	m
J	cost functional	s
P	tire longitudinal force	N
P_x	weighting factor (100)	$-/m^2$
r_c	rollcentre-height at centre of gravity	m
T	tire saturation	-
u_1	front wheel steerrate	deg/s
u_2	longitudinal force	kN
x_1	car yaw angle	-
x_2	car yawrate	$-/s$
x_3	lateral velocity centre of gravity	m/s
x_4	longitudinal velocity centre of gravity	m/s
x_5	lateral position centre of gravity	m
x_6	longitudinal position centre of gravity	m
x_7	front wheel steer angle	deg
$\alpha_{f,r}$	front and rear slip angles	deg
ρ	air density (1.25)	kg/m^3
1, 2, 3, 4	left-front, right-front, left-rear, and right-rear tire	

Table 2. Car data.

		RWD	FWD	
mass	M	650	1200	kg
Yaw moment of inertia	I	1000	2500	kgm^2
Weight distribution f/r	p_f/p_r	0.33/0.67	0.67/0.33	-
Rollstiffness distribution f/r	$a/(1-a)$	0.50/0.50	0.55/0.45	-
Brake force distribution f/r	K_f/K_r	0.50/0.50	0.67/0.33	-
Trackwidth front	t_f	1.8	1.58	m
Trackwidth rear	t_r	1.6	1.58	m
Wheelbase	wb	2.5	2.78	m
Rollcentre height front	r_{cf}	0	0.09	m
Rollcentre height rear	r_{cr}	0.07	0.18	m
CofG height	h	0.2	0.55	m
Frontal surface	A	1.4	1.6	m^2
Drag coefficient	C_d	0.8	0.3	-
Front downforce coefficient	C_f	0.5	0	-
Rear downforce coefficient	C_r	1.0	0	-

The tire lateral forces F_y appearing in the equations of motion are calculated using part of the Magic Formula representation [6]. The effect of longitudinal force on tire saturation is taken into account by adding a term representing a friction ellipse [3], as represented by Equation (11). The resulting expression for the tire lateral force reads

$$F_y(\alpha,F_z,P) = F(\alpha,F_z)T(F_z,P) \tag{8}$$

where

$$F(\alpha,F_z) = D\sin\left[C\,\text{atan}\left[B\alpha - E\{B\alpha - \text{atan}(B\alpha)\}\right]\right] \tag{9}$$

$$D = a_1F_z^2 + a_2F_z \tag{10a}$$

$$C = a_0 \tag{10b}$$

$$B = \frac{a_3}{(a_0a_2)} \qquad B = \frac{a_3}{CD}\sin\left(2\,\text{atan}\left(\frac{F_z}{a_4}\right)\right) \tag{10c}$$

$$E = a_6F_z + a_7 \tag{10d}$$

$$T(F_z,P) = \sqrt{\left(1 - \frac{P^2}{\left(a_1F_z^2 + a_2F_z\right)^2} + \frac{P^2}{\left(a_3 180/\pi\right)^2}\right)} \tag{11}$$

The two expressions for B apply to the different car configurations as can be seen from the tire coefficients listed in Table 3. The slip angles of the left and

Table 3. Tire coefficients.

| | RWD | | FWD |
	Front	Rear	Front/Rear
a_0	1.9	1.9	1.65
a_1	-50	-25	-42
a_2	1500	1500	1200
a_3	450	450	950
a_4	-	-	8.85
a_6	0	0	-0.016
a_7	-6	-6	-0.025

right-hand tires on the same axle are assumed to be identical. The front axle slip angle α_f is approximated by

$$\alpha_f \approx x_7 - \frac{l_f x_2 + x_3}{x_4} \frac{180}{\pi} \qquad (13)$$

while the rear axle slip angle α_r is approximated by

$$\alpha_r \approx \frac{l_r x_2 - x_3}{x_4} \frac{180}{\pi} \qquad (14)$$

The normal forces acting upon the tires are modeled in a quasi-static way and include such quantities as lateral and longitudinal weight transfer, rollstiffness distribution and aerodynamic forces. They are modeled as

$$F_{z1,2} = 0.5 Mgp_f + 0.25 \rho C_f A x_4^2 - 500(K_f + K_r)u_2 \frac{h}{wb}$$

$$\pm \left(F_{y1} + F_{y2} + F_{y3} + F_{y4}\right)(h - r_c)\frac{a}{t_f} \pm \left(F_{y1} + F_{y2}\right)\frac{r_{cf}}{t_f} \qquad (15)$$

for left and right front tires, respectively, and

$$F_{z3,4} = 0.5 Mgp_r + 0.25 \rho C_r A x_4^2 + 500(K_f + K_r)u_2 \frac{h}{wb}$$

$$\pm \left(F_{y1} + F_{y2} + F_{y3} + F_{y4}\right)(h - r_c)\frac{(1 - a)}{t_r} \pm \left(F_{y3} + F_{y4}\right)\frac{r_{cr}}{t_r} \qquad (16)$$

for left and right rear tires, respectively. Aerodynamic drag F_a is represented by

$$F_a = 0.5 \rho C_d A x_4^2 \qquad (17)$$

2.2. Cost Functional

In order to arrive at a unique solution, the car is supposed to complete the manoeuvre as quick as possible. This is achieved by minimizing the following functional

$$J(u(t),t) = \int_{t_0}^{t_f} dt \qquad (18)$$

which represents the time the car requires to complete the manoeuvre while it is subjected to driver actions $u(t)$. Symbols t_0 and t_f denote the time at the start and the end of the manoeuvre, respectively.

2.3. Control Constraints

Both control functions i.e. the front wheel steer rate u_1 and the longitudinal force u_2 are limited in magnitude [7]; the front wheel steer rate is assumed to be limited by the driver's capabilities and the longitudinal force is limited either by the maximum performance of the driveline or by the maximum adhesion between the tires and the road. The driver limit is taken into account by limiting the steer rate to a fixed maximum. The driveline limit is taken into account by limiting the value of the traction force to the maximum traction force that can be generated by the driveline. This maximum force is calculated as a function of forward velocity by reformulating the engine's torque versus angular velocity curve into a longitudinal force versus forward velocity relation, using the total gear ratios and the wheel radius. The maximum adhesion between the tires and the road is taken into account by limiting the maximum longitudinal force, allocated to each individual tire, to the product of the tire's friction coefficient and normal force. The corresponding total longitudinal force is then divided over front and rear axles using proportionality factors K_f and K_r. After this, the front and rear axle forces are split equally onto left and right wheels.

2.4. State Constraints

The values of the state variables are limited by the fact that the car has to stay on the road. This is taken into account by forcing the car's centre of gravity to stay within the boundaries of the road. This is achieved by expanding the cost functional J with an extra term whose value depends on the distance between the centre of gravity and the road centerline. The expanded cost functional then becomes

$$J(u(t),t) = \int_{t_0}^{t_f} (g_x(x_5,x_6)H(g_x) + 1)dt \qquad (19)$$

in which $g_x(x_5, x_6)$ represents the square value of the distance between the car's centre of gravity and the road centerline. The step function $H(g_x)$ indicates whether or not the car's centre of gravity exceeds its limits; if a limit is exceeded

$H(g_x) = P_x$ ($P_x > 0$), if no limit is exceeded $H(g_x) = 0$. Minimization of this functional will cause the cente of gravity position to exceed its boundaries only minimally, which implies that the car stays on the road. For the cases considered, the road is a lane-change with a lateral displacement of 8.5 metres occurring over a track length of approximately 30 metres. The centerline of this road is represented by [4]

$$x_c = 4.25 \, \text{erf}((x_6 - 40)/11.3) + 4.25 \tag{20}$$

where *erf* denotes the integral of the Gaussian distribution function from 0 to x, also known as the error function. The width of the road ranges from 1.8 to 2 metres.

2.5. Change of Independent Variable

To simplify the solution process of this optimal control problem, the independent variable time t is replaced by a new independent variable s: the distance travelled along the road centerline. In order to make this change, the relationship between time and travelled distance along the road centerline has to be used

$$dt = ds/V \tag{21}$$

where V denotes the momentary velocity of the car's centre of gravity along the road centerline. In determining the infinitesimal distance ds, it has to be taken into account that this is not a constant but that its value depends upon the position of the centre of gravity relative to the track, as shown in Fig. 2.

From Fig. 2, it is easily seen that the following relation exists

$$ds = ds' \pm d \tan(b) \tag{22}$$

where *b* is the angle between consecutive road centerline parts while the sign of
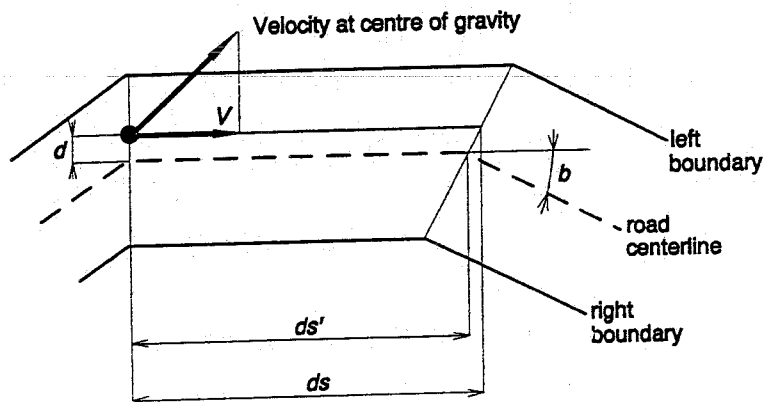
ds': distance between centerline points

ds: distance to be travelled

V: projection of velocity onto road centerline

d: distance between centre of gravity and road centerline

Fig. 2. Schematic representation of road with velocity of centre of gravity and distance to be travelled.

the last term in this expression is determined by the position of the centre of gravity relative to the course of the road. Velocity V is calculated by taking the inner product of the centre of gravity's velocity vector $[x_5, x_6]^T$ and the unity vector in the direction of the track centerline $[r_x, r_y]^T$ and reads

$$V = r_x \dot{x}_6 + r_y \dot{x}_5 \qquad (23)$$

To complete the change of independent variable, the equations of motions expressed by Equations (1) through (7) and the functional from Equation (19) have to be reformulated, using Equation (21).

The reformulated optimal control problem was solved by applying the Gradient algorithm [8,9]. This algorithm calculates improved control functions based on the linearization of the expanded cost functional around the current control and state functions. It involves the backward integration of a set of first order differential equations that yield the time-histories of the so-called Lagrange multipliers, which guarantee the satisfaction of the equations of motion. These Lagrange multipliers are then used to calculate new control functions that will cause the value of the functional to decrease. The formulation of the optimal control problem presented here and the Gradient algorithm were implemented in a computer program which was executed on a workstation.

3. RESULTS AND DISCUSSIONS

Using the optimal control formulation of the problem under consideration, a number of cases were simulated. Here, two of these cases are presented. The main differences between these two cases lie in the different car configurations and different entry speeds. In the first case, a rear wheel drive (RWD) car, with car and tire data similar to that of a Formula One race car (see Tables 2 and 3), enters the lane-change with a forward velocity of 30 metres per second. In the second case, a front wheel drive (FWD) car, with car and tire data similar to those of a medium-size passenger car (see Tables 2 and 3), enters the lane-change with a forward velocity of 55 metres per second. To accommodate this high entry speed, the entry section of the lane-change was extended by 30 metres.

The most important results of these two simulations are shown in Figs. 3 and 4, respectively. Both figures contain five graphs. These graphs show as a function of travelled distance along the lane-change centerline:

(1) the car's center of gravity position and attitude relative to the road
(2) the front wheel steer angle
(3) the longitudinal force
(4) the slip angles front and rear
(5) the tire saturation, which is the ratio of generated and maximum tire forces

Fig. 3. Car centre of gravity position relative to road, steer angle, longitudinal force, slip angles, and tire saturation as a function of travelled distance along the road centerline, for rear wheel drive car.
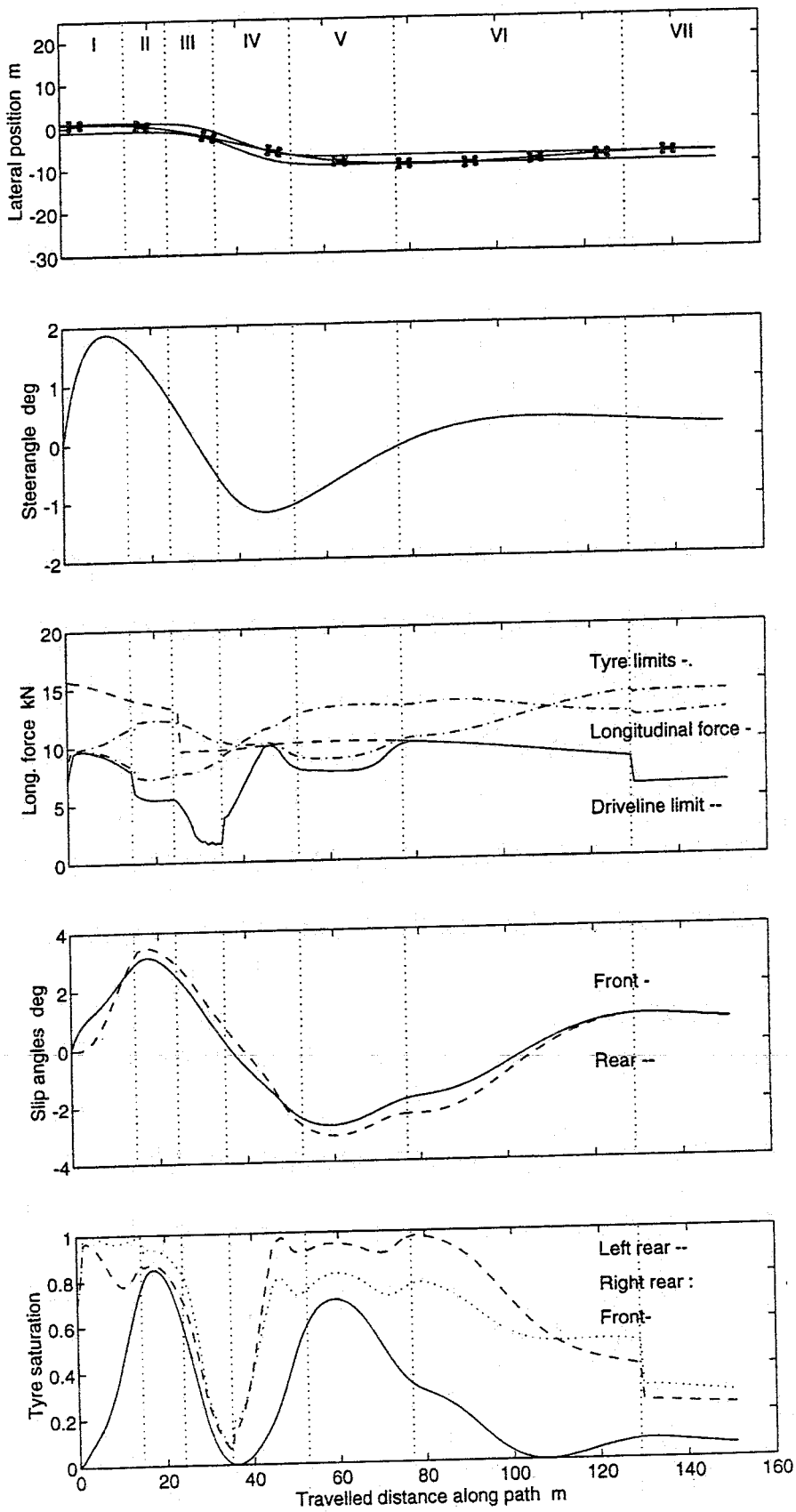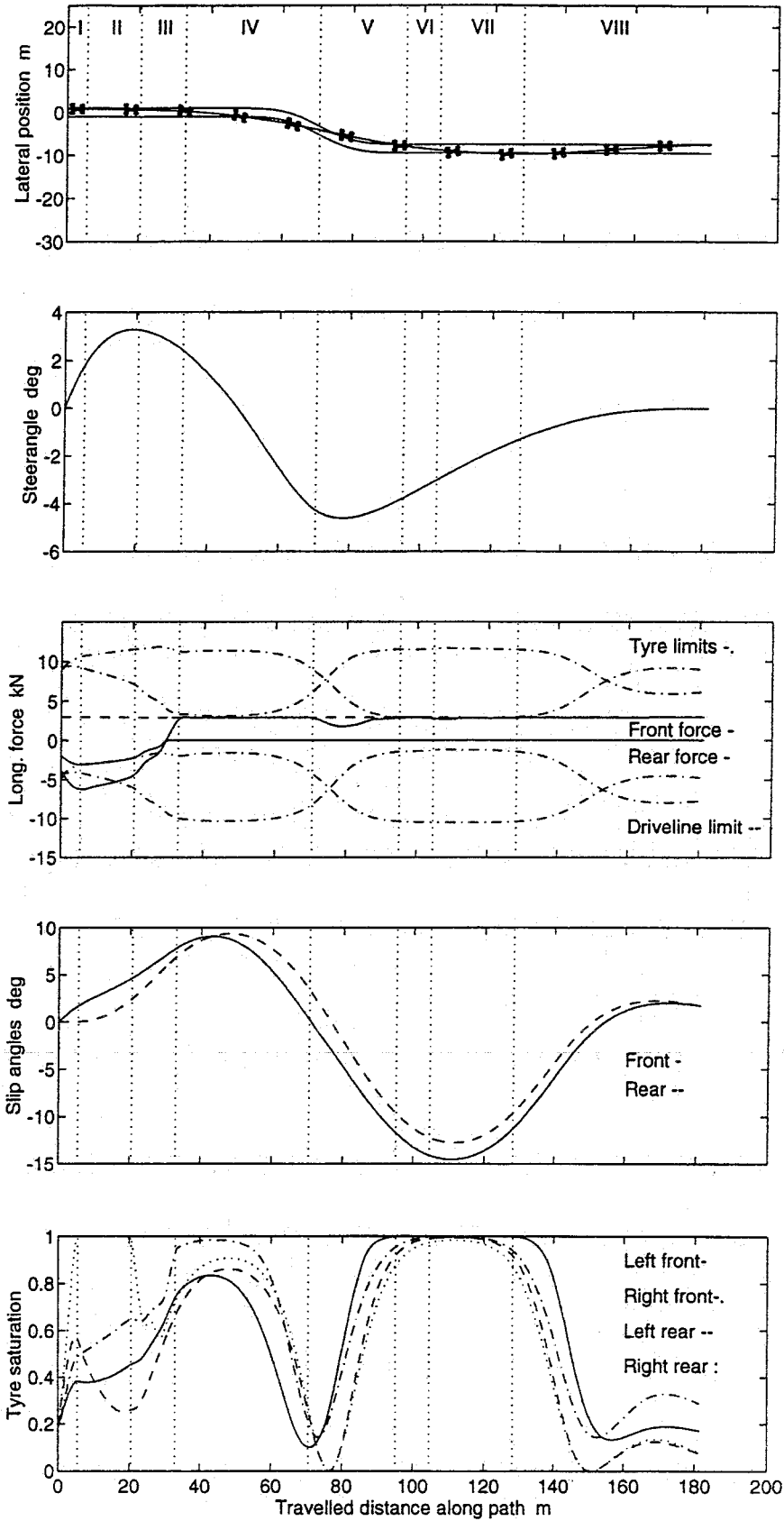
Fig. 4. Car centre of gravity position relative to road, steer angle, longitudinal force, slip angles, and tire saturation as a function of travelled distance along the road centerline, for front wheel drive car.

In each graph, dividing lines are shown to indicate the transition from one stage of the manoeuvre to another. The times the cars required to complete the lane-changes were 3.35 and 3.46 seconds for the RWD and FWD cars, respectively.

3.1. Rear Wheel Drive Car

The results obtained with the rear wheel drive car are discussed for the seven stages (I to VII) indicated in Fig. 3.

Stage I   The steer angle is increased to enter the car into the right-hand turn, while the rear tires produce their maximum traction force (limited by tire-road adhesion). The rear tires are saturated with longitudinal force while the front tires are hardly saturated.

Stage II   The steer angle is decreased in anticipation of the left-hand turn, while the traction force is decreased to allow the rear tires to produce lateral forces. The rear tires are saturated with a combination of lateral and longitudinal forces, while the front tires are less saturated with lateral force alone.

Stage III The steer angle changes sign as the car starts its transition from the right-hand into the left-hand turn, while the traction force almost vanishes to allow the rear tires to produce even greater lateral forces to prevent the car from turning too far to the right. Both front and rear tire saturation decreases.

Stage IV   The steer angle is increased to enter the car into the left-hand turn. As soon as the front slip angle changes sign, the traction force suddenly increases to its maximum value (limited by the driveline). In doing so, the rear tires are instantly saturated with traction force, which causes the rear lateral forces to almost vanish. This increases yaw velocity and turns the car into the left-hand bend even more.

Stage V   The steer angle is decreased to keep the car on the road, while the traction force does not hold its maximum value to allow the rear tires to produce lateral forces. The rear tires are saturated with a combination of traction and lateral forces, while the front tires are less saturated with lateral forces alone.

Stage VI   The steer angle changes sign again; the corresponding steering wheel angle would now be turned to the right in a left-hand corner, indicating opposite-lock. In doing so, the car is prevented from turning too far to the left at the end of the lane-change. The rear tires are saturated considerably with a combination of lateral and longitudinal forces.

Stage VII The steer angle is maintained, while the maximum traction force (limited by the driveline) is applied. At the beginning of this period, the driveline limit is decreased suddenly as a result of a necessary gearchange. Rear tire saturation is caused by longitudinal force and decreases because of the driveline limit and the increase of normal force at increasing velocity. Front tire saturation is negligable.

3.2. Front Wheel Drive Car

The results obtained with the front wheel drive car are discussed for the eight stages (I to VIII) indicated in Fig. 4.

Stage I   The steer angle is increased to enter the car into the right-hand turn, while a brake force (negative longitudinal force) is applied. This brake force is less than the maximum brake force possible in order to allow the front tires to produce sufficient lateral forces to enter the car into the turn. All four tires are marginally saturated.

Stage II   The steer angle is still increased to enter the car into the right-hand turn, while the maximum brake force (limited by right rear-tire adhesion) is applied. The right-rear tire is completely saturated with the brake force, while the other tires are still marginally saturated.

Stage III   The steer angle is decreased, while the longitudinal force switches from maximum brake force to maximum traction force (limited by the driveline). When the longitudinal force changes sign, the yawrate is reduced to prevent the car from turning too far to the right. Tire saturation increases except for the right-rear tire.

Stage IV   The steer angle changes sign as the car starts its transition from the right-hand into the left-hand turn, while maximum traction force (limited by the driveline) is applied. At the beginning of this stage, the right-front tire is saturated almost completely, while the other tires are saturated considerably. At the end of this stage, tire saturation decreases for all tires because of the decrease of lateral forces.

Stage V   The steer angle reaches its maximum negative value and after that decreases to prevent the car from turning too far to the left. The traction force decreases to allow the front tires to produce sufficient lateral force to enter the car into the left-hand turn and afterwards returns to its maximum. At the beginning of this stage, tire saturation clearly shows the transition from right-hand to left-hand turn. At the end of this stage, all tires are saturated almost completely.

Stage VI   The steer angle is decreased, while the maximum traction force is applied (limited by the driveline and left-front tire adhesion). Tire saturation is almost complete for all four tires.

Stage VII   The steer angle is still decreased, while the traction force is slightly decreased to allow the front tires to produce more lateral force to prevent the car from running wide. At the beginning of this stage, tire saturation is almost complete. At the end of this stage, tire saturation decreases because of the decrease in lateral forces as the car heads out onto the straight.

Stage VIII   The steer angle vanishes, while the maximum traction force (limited by the driveline) is still applied. Tire saturation decreases because of the decrease in lateral forces as the car is almost running straight ahead.

4. CONCLUSIONS

This paper presents a method to calculate the driver actions which are required for a car to perform specified manoeuvres in as short a time as possible. This method uses non-linear car and tire models, is based on the optimal control theory, and uses the Gradient method to solve the resulting equations. Results are presented, in which two different cars perform similar lane-changes which are defined by a road the car is to stay on. Results clearly show different driving strategies for front and rear wheel drive cars due to the significant effect of longitudinal force on tire saturation. These results imply that the optimal control theory can be used to optimize car handling by means of inverse simulation, when using non-linear car and tire models.

REFERENCES

[1] Fujioka, T., Kimura, T., "Numerical simulation of minimum-time cornering behaviour", JSAE Review, Volume 13, no. 1, 1992, pp. 44-51.
[2] Bernard, J., Pickelmann, M., "An inverse linear model of a vehicle", Vehicle System Dynamics, Volume 15, 1986, pp. 179-186.
[3] Hatwal, H., Mikulcik, E.C., "Some inverse solutions to an automobile path-tracking problem with input control of steering and brakes", Vehicle System Dynamics, Volume 15, 1986, pp. 61-71.
[4] Sridhar, J., Hatwal, H., "A comparative study of four wheel steering models using the inverse solution", Vehicle System Dynamics, Volume 21, 1992, pp. 1-18.
[5] Trom, J.D., Vanderploeg, M.J., Bernard, J.E., "Application of inverse models to vehicle optimization problems", Vehicle System Dynamics, Volume 19, 1990, pp. 97-110.
[6] Bakker, E., Pacejka, H.B., Lidner, L., "A new tire model with an application in vehicle dynamics studies", SAE-Paper 890087.
[7] Mufti, I.H., Computational methods in optimal control, Springer, Berlin, 1970.
[8] Sage, A.P., Optimum systems control, Prentice-Hall, New-Jersey, 1968.
[9] Kirk, D.E., Optimal control theory, Prentice-Hall, New-Jersey, 1970.